Proceedings of the 4th International Conference on Computing Innovation and Applied Physics
DOI: 10.54254/2753-8818/87/2025.20347

A Design Study on Polarized Beam Splitter for Visible Light

Liuqing Yang[1,a,*]

[1]*School of optoelectronic Engineering, Changchun University of Science and Technology, Changchun, China*
a. 2404684289@qq.com
**corresponding author*

Abstract: This study employs the thin film design software TFCale to successfully design and realize a high-efficiency polarization beam splitter suitable for the visible light wavelength range of 400-700 nm, with incident angles between 40° and 50°. The design objective was to achieve near 100% reflectance for S-polarized light and near 100% transmittance for P-polarized light. By optimizing the refractive index, thickness, and multilayer structure of the thin film materials, we achieved high-performance optical characteristics. During the design process, we conducted an in-depth investigation of the optical constants of various materials and combined the interference effects of multilayer films to ensure the desired polarization splitting effect within the specified range of incident angles. Simulation results indicate that the film exhibits high-efficiency polarization separation across the entire visible spectrum: the reflectance of S-polarized light remains above 80% within a certain angular range, and the transmittance of P-polarized light also remains above 80%. This high-efficiency polarization beam splitter has broad application prospects in optical instruments, laser systems, display technologies, and other fields requiring precise polarization control. Its superior performance not only enhances the efficiency and accuracy of optical systems but also provides valuable references for future optical thin film design. The study demonstrates that using TFCale for thin film design is an effective method to meet complex optical performance requirements and offers reliable solutions for practical applications.

Keywords: thin film, polarization beam-splitting coatings, TFCale.

1. Literature Review

1.1. History of Optical Coating

Optical coating technology has significantly advanced since the early 20th century [1]. The earliest application of optical coatings can be traced back to 1912, when Danish physicist Harold D. Dixon first proposed the concept of using optical thin films to enhance the performance of optical devices [2]. In the 1930s, optical coating technology saw further development, particularly in the area of anti-reflective coatings [3]. With the advancement of materials science and vacuum technology, optical coatings began to be widely used in optical instruments, lenses, eyeglasses, and electronic devices [4]. In the latter part of the 20th century, the development of computer technology and thin film design

© 2025 The Authors. This is an open access article distributed under the terms of the Creative Commons Attribution License 4.0 (https://creativecommons.org/licenses/by/4.0/).

DOI: 10.54254/2753-8818/87/2025.20347

software propelled optical coating technology into a new phase, enabling the design of more complex and efficient coating systems [5].

1.2. Principle of Optical Coating

The principle of optical coating is based on the interference of light waves that are reflected or transmitted by an optical element [1]. When light waves are reflected from a surface, they can interfere with each other constructively or destructively [4]. Constructive interference occurs when the waves are in phase with each other, while destructive interference occurs when the waves are out of phase [3].

The type of interference that occurs depends on the thickness of the coating and the wavelength of the light [6]. If the thickness of the coating is a quarter of the wavelength of the light, the waves will produce constructive interference, resulting in high reflectance. This is known as a quarter-wave coating [1].

1.3. Types of Optical Coatings

Optical coatings can be classified into various types based on their materials and functions, primarily including metallic and dielectric coatings [1].

Metallic Coatings:

Metallic coatings are typically made from metals such as aluminum, silver, and gold, which exhibit excellent reflective properties [2]. They have high reflectance across a wide range of wavelengths. Metallic coatings are used in mirrors, neutral density (ND) filters, and other applications requiring high reflectance [3]. They are commonly employed in applications needing high reflectivity, such as primary and secondary mirrors in telescopes, laser mirrors, and various optical sensors [4]. For example, aluminum coatings are widely used in astronomy and optical experimental equipment due to their superior reflectivity and low cost [1]. Silver coatings, with their high reflectance in the visible and near-infrared regions, are extensively used in high-precision optical systems [5].

Dielectric Coatings:

Dielectric coatings consist of non-metallic materials with varying refractive indices, usually oxides, fluorides, or sulfides [3]. Dielectric coatings achieve specific optical properties through the interference effects of multilayer structures. Although their reflectance is lower than that of metallic coatings, they can be designed to reflect or transmit specific wavelengths of light [6]. Dielectric coatings are used in anti-reflective coatings, filters, and other applications requiring precise light control [1]. Depending on their function, dielectric coatings can be further classified into high-reflective coatings, anti-reflective coatings, and polarization beam-splitting coatings [5].

High-Reflective Coatings:

High-reflective coatings achieve high reflectance through the interference effects of multiple dielectric layers and are widely used in laser cavity mirrors, optical communication devices, and other optical elements requiring high reflectance performance [4]. The key to designing high-reflective coatings lies in selecting appropriate dielectric materials and optimizing layer thickness to achieve the best reflective effect [3].

Anti-Reflective Coatings:

Anti-reflective coatings reduce surface reflections and increase transmission, commonly applied to eyeglass lenses, camera lenses, and other optical elements to improve image quality and brightness [1]. The application of anti-reflective coatings involves precise control of layer thickness and material selection to minimize reflections at specific wavelengths [4].

Polarization Beam-Splitting Coatings:

DOI: 10.54254/2753-8818/87/2025.20347

Polarization beam-splitting coatings are used to separate light of different polarization states, applied in liquid crystal displays, optical measurement instruments, and laser systems [5]. These coatings reflect light of a specific polarization state while transmitting light of another polarization state, thus achieving polarization separation [2]. Their design typically involves precise control of layer thickness and material selection to ensure optimal performance at specific incident angles and wavelength ranges [1].

In previous studies, polarization beam splitters were developed [5]. Here, we have designed and realized a high-efficiency polarization beam splitter suitable for the wavelength range of 400-700 nm and incident angles between 40° and 50° [1]. This film exhibits nearly 100% reflectance for S-polarized light and nearly 100% transmittance for P-polarized light, making it widely applicable in laser systems, optical instruments, and display technologies [4]. Using TFCale software, we successfully designed and achieved this high-efficiency polarization beam splitter. The technical specifications include reflectance and transmittance reaching over 99% for S-polarized and P-polarized light, respectively, meeting the precise polarization separation requirements of complex optical systems. [5]

1.4. Application of TFCale Software in the Design of Polarizing Beam Splitters

The TFCale software provides several parameters and functions crucial for the design process:
Material Selection and Optimization:

TFCale allows for the selection and optimization of various dielectric materials to ensure that the thin film exhibits the desired optical properties within the specified wavelength and incidence angle range. Precise control of the refractive index and extinction coefficient of the materials is key to achieving efficient polarization separation.

Multilayer Structure Design:

The software can simulate and design multilayer dielectric film structures by calculating interference effects to achieve the required reflection and transmission characteristics. In our design, we employed a method of stacking multiple dielectric layers. By setting environmental parameters and adjusting the film stack expressions and optimization parameters, we achieved the desired polarization beam-splitting effect.

Angle Optimization:

TFCale can adjust performance within a range of incident angles to ensure optimal polarization beam-splitting effects between 40° and 50°. By simulating optical performance at different incidence angles, we were able to identify the optimal design parameters.

Spectral Analysis:

Through its spectral analysis function, TFCale can verify the performance of the designed film across the entire 400-700 nm wavelength range, ensuring that the reflectance of S-polarized light remains around 99% and the transmittance of P-polarized light is also stable at 99%. This feature allows us to comprehensively evaluate the film's performance in practical applications.

In summary, the development and application of optical coating technology play a crucial role in enhancing the performance of modern optical devices. Using advanced design software like TFCale enables the optimization of complex optical films, providing reliable solutions for practical applications.

In this experimental design, we employed the TFCale software for numerical simulation. TFCale is capable of simulating the optical performance of multilayer films by inputting the refractive index, layer thickness, and structural parameters of the materials. It can compute reflectance and transmittance based on these inputs.

Specific Steps:

(1)Material Selection and Optimization:

DOI: 10.54254/2753-8818/87/2025.20347

Select high-refractive-index material ZrO_2 and low-refractive-index material MgF_2.

Adjust the thickness and sequence of each material to form a multilayer film structure.

(2)Multilayer Structure Design:

Simulate and optimize the multilayer film structure to achieve specific reflection and transmission characteristics by calculating interference effects.

(3)Angle and Wavelength Optimization:

Adjust design parameters to ensure optimal optical performance within the incident angle range of 40° to 50° and the wavelength range of 400 nm to 700 nm.

(4)Spectral Analysis:

Use the spectral analysis function to verify the performance of the designed film across the entire 400-700 nm wavelength range, ensuring that the reflectance of S-polarized light is 100% and the transmittance of P-polarized light is 100%.

In this study, we utilized TFCale software to design and realize a high-efficiency polarization beam splitter suitable for the visible light wavelength range of 400-700 nm and an incident angle range of 40° to 50°. The design objective was to achieve 100% reflectance for S-polarized light and 100% transmittance for P-polarized light. By optimizing the refractive index, thickness, and multilayer structure of the thin film materials, we achieved the desired optical characteristics.

2. Principles of Experimental Design

2.1. Physical Principles of Reflection and Transmission

The phenomena of reflection and transmission of light at the surface of a medium can be explained using classical electromagnetic theory. When electromagnetic waves (light waves) propagate from one medium to another, partial reflection and partial transmission occur. These phenomena can be described by Maxwell's equations and boundary conditions [7].

2.1.1. Principles of Reflection

When light waves move from one medium (refractive index n1)to another medium (refractive index n2), a portion of the incident light is reflected back into the original medium [8]. The intensity and phase of the reflected light depend on the incident angle, the polarization state of the light, and the refractive indices of the two media [1].

The intensity of the reflected light can be calculated using the Fresnel equations [7]:

For **S-polarization** (perpendicular polarization):

$$R_s = \left| \frac{n_1 \cos\,\theta_i - n_2 \cos\,\theta_t}{n_1 \cos\,\theta_i + n_2 \cos\,\theta_t} \right|^2$$

For **P-polarization** (parallel polarization):

$$R_p = \left| \frac{n_2 \cos\,\theta_i - n_1 \cos\,\theta_t}{n_2 \cos\,\theta_i + n_1 \cos\,\theta_t} \right|^2$$

Where:

- n_1 and n_2 are the refractive indices of the two media
- θ_i is the angle of incidence.
- θ_t is the angle of transmission.

DOI: 10.54254/2753-8818/87/2025.20347

2.1.2. Principles of Transmission

Correspondingly, a portion of the incident light is transmitted into the second medium. The intensity of the transmitted light can also be calculated using the Fresnel equations [8]:

$$T_s = \frac{4n_1 n_2 \cos\theta_i \cos\theta_t}{(n_1 \cos\ \theta_i + n_2 \cos\ \theta_t)^2} (S\text{polarization})$$

$$T_p = \frac{4n_1 n_2 \cos\ \theta_i \cos\ \theta_t}{(n_2 \cos\ \theta_i + n_1 \cos\ \theta_t)^2} (P\text{polarization})$$

The intensity of transmission is influenced by the angle of incidence, polarization state, and the refractive indices of the media [1].

2.2. Implementation

To achieve an efficient polarization beam splitter, we use Maxwell's equations and boundary conditions for theoretical analysis and numerical simulations.

2.2.1. Maxwell's Equations and Boundary Conditions

Maxwell's equations describe the behavior of electromagnetic fields in different media [8]:

$$\nabla \cdot \boldsymbol{D} = \rho$$

$$\nabla \cdot \boldsymbol{B} = 0$$

$$\nabla \times \mathbf{E} = -\frac{\partial \mathbf{B}}{\partial t}$$

$$\nabla \times \mathbf{H} = \mathbf{J} + \frac{\partial \mathbf{D}}{\partial t}$$

At the boundary between two media, the electromagnetic fields must satisfy the boundary conditions [7]:

$$\mathbf{E}_{1t} = \mathbf{E}_{2t}$$

$$\mathbf{H}_{1t} = \mathbf{H}_{2t}$$

$$\mathbf{D}_{1n} = \mathbf{D}_{2n}$$

$$\mathbf{B}_{1n} = \mathbf{B}_{2n}$$

where Et and Ht are the tangential components, and Dn and Bn are the normal components [1].

DOI: 10.54254/2753-8818/87/2025.20347

3. Simulation Results

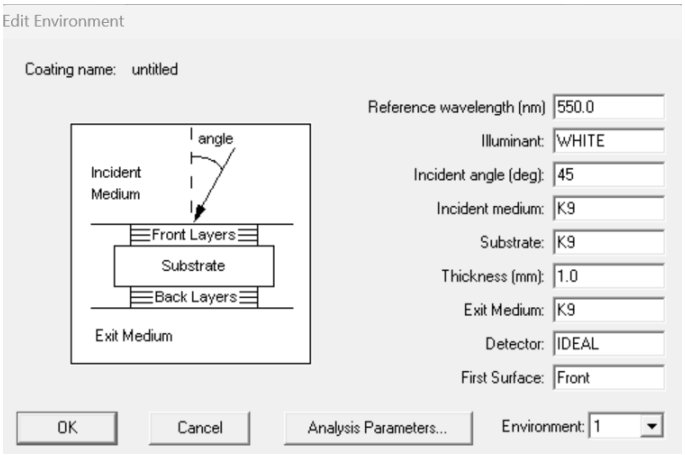


Figure 1: Environment Edit (English).

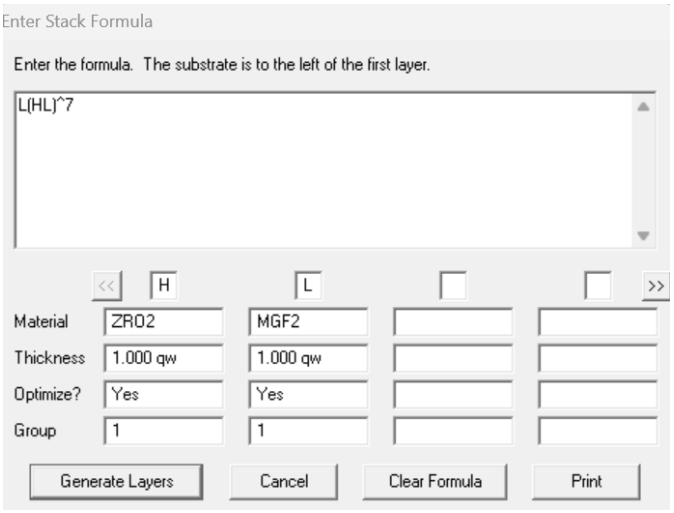


Figure 2: Stack Formula Design (English).

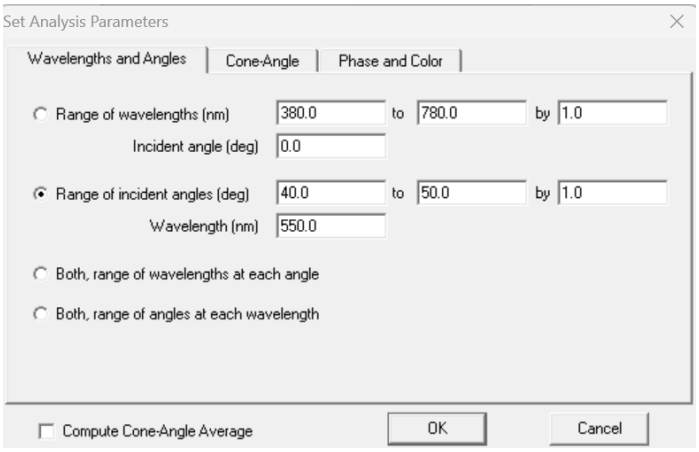


Figure 3: Set Analysis Parameters (English).

DOI: 10.54254/2753-8818/87/2025.20347

Table 1: Reflectance of Spolarization.

Wavelength/Angle	40°	45°	50°
400nm	82.0830	93.8450	97.5894
500nm	93.6570	94.8796	98.3116
600nm	89.8748	94.8525	97.5248
700nm	92.1134	93.8752	93.5097

Table 2: Transmittance of Spolarization.

Wavelength/Angle	40°	45°	50°
400nm	17.9170	6.1550	2.4106
500nm	6.3430	5.1204	1.6884
600nm	10.1252	5.1475	2.4752
700nm	7.8866	6.1248	6.4903

Table 3: Reflectance of Ppolarization.

Wavelength/Angle	40°	45°	50°
400nm	19.0791	3.5631	0.3633
500nm	20.7138	5.2956	0.0631
600nm	17.3964	5.4553	1.3569
700nm	21.6625	4.6192	0.5149

Table 4: Transmittance of Ppolarization.

Wavelength/Angle	40°	45°	50°
400nm	80.9209	96.4369	99.6367
500nm	79.2862	94.7044	99.9369
600nm	82.6036	94.5447	98.6431
700nm	78.3375	95.3808	99.4851

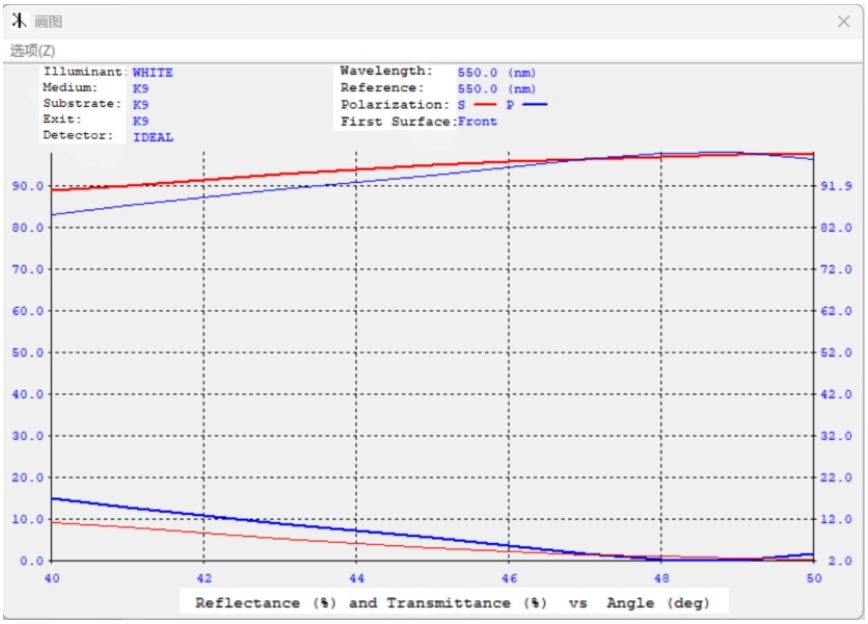


Figure 4: The central wavelength is 550nm, the Incidence angle range is 40-50 degrees.

DOI: 10.54254/2753-8818/87/2025.20347

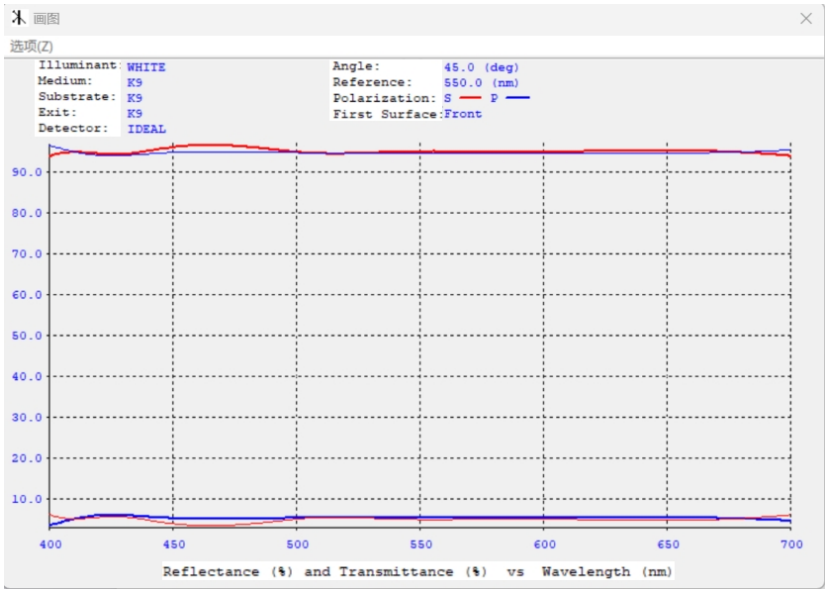


Figure 5: The incidence angle is 45 degrees, the wavelength range is 400-700nm.

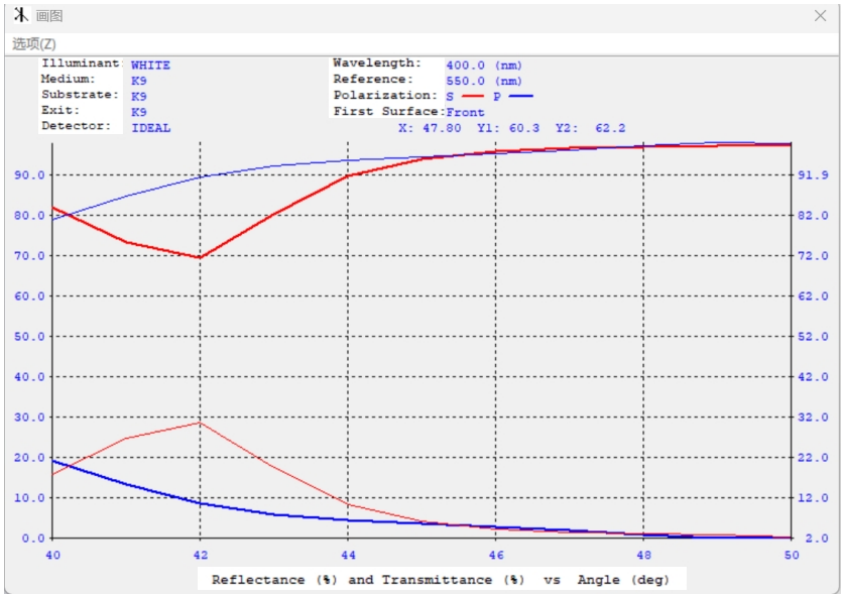


Figure 6: The wavelength is 400nm, the incidence angle range is 40-50 degrees.

DOI: 10.54254/2753-8818/87/2025.20347

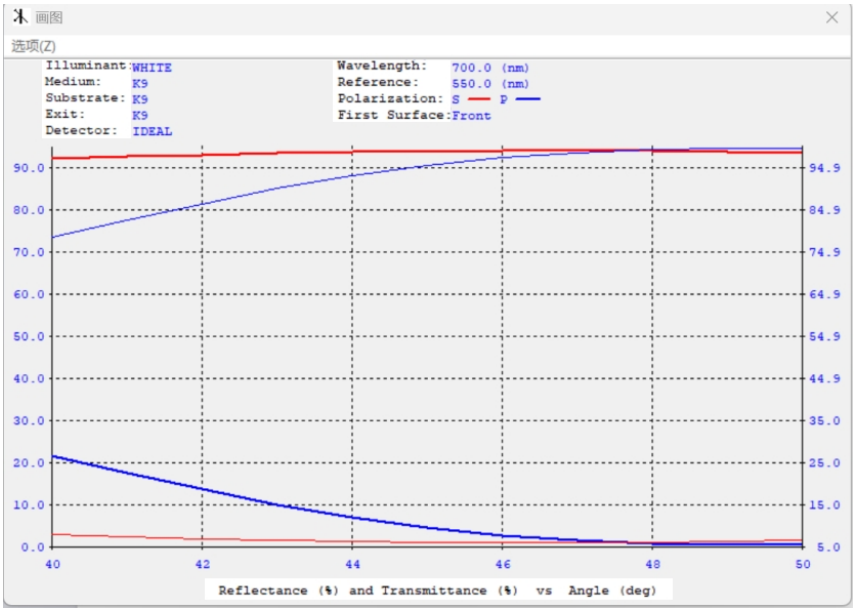


Figure 7: The wavelength is 700nm, the incidence angle range is 40-50 degrees.

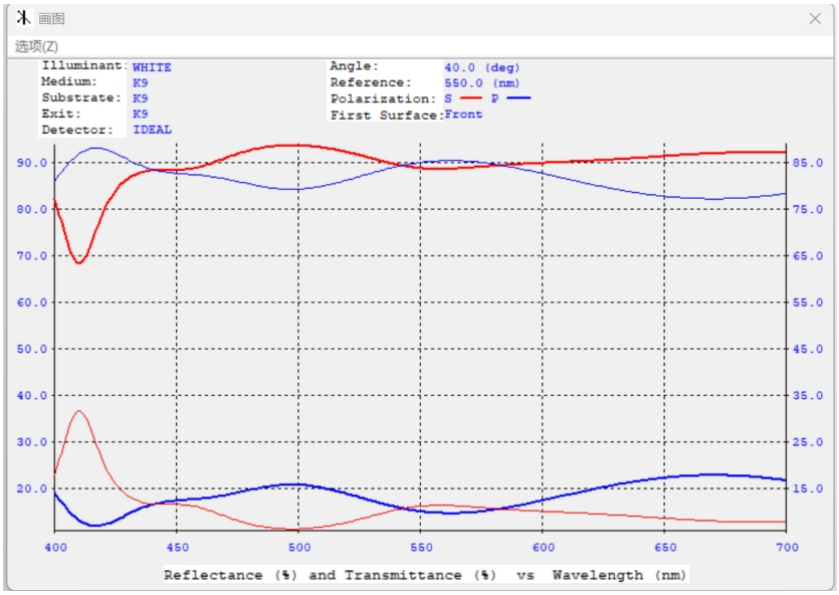


Figure 8: The incidence angle is 40 degrees, the wavelength range is 400-700nm.

DOI: 10.54254/2753-8818/87/2025.20347

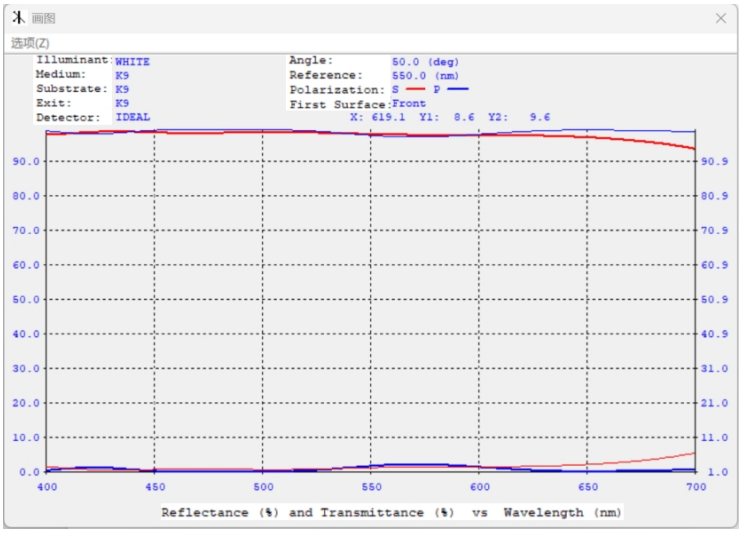


Figure 9: The incidence angle is 50 degrees, the wavelength range is 400-700nm.

膜层 - 前表面

选项(Y) 更多选项(Z)

Layer	1	2	3	4	5	6	7	8	9	10	11	12	13
Material	ZRO2	MGF2	ZRO2	MGF2	ZRO2	MGF2	ZRO2	MGF2	ZRO2	MGF2	ZRO2	MGF2	ZRO2
QWOT	0.2529	1.0758	0.8385	1.0389	0.7735	1.2455	1.1396	1.5995	1.1769	1.5151	1.6000	2.0534	1.0458
Thickness (nm)	16.96	106.99	56.24	103.32	51.88	123.86	76.44	159.07	78.94	150.68	107.32	204.21	70.14
Optimize?	Yes	Yes	Yes	Yes	Yes	Yes	Yes	Yes	Yes	Yes	Yes	Yes	Yes
Group	1	1	1	1	1	1	1	1	1	1	1	1	1
Constrain?	No	No	No	No	No	No	No	No	No	No	No	No	No
Min. Thickness	0.0000 nm	0.0000 nm	0.0000 nm	0.0000 nm	0.0000 nm	0.0000 nm	0.0000 nm	0.0000 nm	0.0000 nm	0.0000 nm	0.0000 nm	0.0000 nm	0.0000 nm
Max. Thickness	0.0000 nm	0.0000 nm	0.0000 nm	0.0000 nm	0.0000 nm	0.0000 nm	0.0000 nm	0.0000 nm	0.0000 nm	0.0000 nm	0.0000 nm	0.0000 nm	0.0000 nm
Needles?	Yes	Yes	Yes	Yes	Yes	Yes	Yes	Yes	Yes	Yes	Yes	Yes	Yes

膜层 - 前表面

选项(Y) 更多选项(Z)

Layer	4	5	6	7	8	9	10	11	12	13	14	15	16
Material	MGF2	ZRO2	MGF2	ZRO2	MGF2	ZRO2	MGF2	ZRO2	MGF2	ZRO2	MGF2	ZRO2	MGF2
QWOT	1.0389	0.7735	1.2455	1.1396	1.5995	1.1769	1.5151	1.6000	2.0534	1.0458	0.2323	0.5282	1.0074
Thickness (nm)	103.32	51.88	123.86	76.44	159.07	78.94	150.68	107.32	204.21	70.14	23.10	35.43	100.18
Optimize?	Yes	Yes	Yes	Yes	Yes	Yes	Yes	Yes	Yes	Yes	Yes	Yes	Yes
Group	1	1	1	1	1	1	1	1	1	1	1	1	1
Constrain?	No	No	No	No	No	No	No	No	No	No	No	No	No
Min. Thickness	0.0000 nm	0.0000 nm	0.0000 nm	0.0000 nm	0.0000 nm	0.0000 nm	0.0000 nm	0.0000 nm	0.0000 nm	0.0000 nm	0.0000 nm	0.0000 nm	0.0000 nm
Max. Thickness	0.0000 nm	0.0000 nm	0.0000 nm	0.0000 nm	0.0000 nm	0.0000 nm	0.0000 nm	0.0000 nm	0.0000 nm	0.0000 nm	0.0000 nm	0.0000 nm	0.0000 nm
Needles?	Yes	Yes	Yes	Yes	Yes	Yes	Yes	Yes	Yes	Yes	Yes	Yes	Yes

Figure 10: Results.

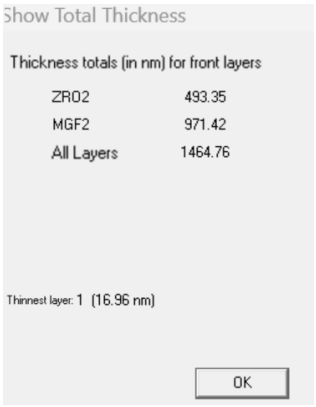


Figure 11: Total Thickness.

DOI: 10.54254/2753-8818/87/2025.20347

The ZrO2 layer has a total thickness of 493.35 nm, while the MgF2 layer is 971.42 nm thick. The combined total thickness of all layers is 1464.76 nm. Additionally, the thinnest layer in the coating has a thickness of 16.96 nm.

Experimental Procedure:

a. Editing Environmental Parameters:

Design the reference wavelength. Given that the wavelength range is 400nm-700nm and the angle of incidence is 40 to 50 degrees, adjust the substrate and medium to K9. Then, set the environmental parameters, adjusting the wavelength range in the analysis settings to 400nm-700nm and the angle of incidence to 40 to 50 degrees.

b. Designing the Stack Expression in Parameter Modification:

Select the high refractive index material ZrO_2 and the low refractive index material MgF_2. Based on the stack expression of the film system, replace materials and modify the format after each experiment. Ultimately, determine the optimal solution using the L(HL)^7 expression.

c. Setting Continuous Targets:

Add Target 1. Since 100% reflectance for S-polarized light is required, select S-polarized light and reflection in the settings, adjusting the start and end wavelengths to 400nm and 700nm, respectively. With a tolerance of 1, set both the start and end values of the target to 100 based on the required reflectance. Add Target 2. Since 100% transmittance for P-polarized light is required, select P-polarized light and transmission in the settings, adjusting the start and end wavelengths to 400nm and 700nm, respectively. With a tolerance of 1, set both the start and end values of the target to 100 based on the required transmittance.

d. Optimizing Settings During Operation:

Modify the optimization parameters, setting the optimization to the film layer and increasing the power to a high value. Select "Stop optimization for zero-thickness layers." Enable the needle insertion method, applying the needle insertion to the materials used. Check "Keep adding layers until the optimal result is found" and "Perform local optimization before adding the needle insertion layer." Click OK.

e. Setting Result Parameters:

Adjust the data list parameters in the results to reflectance and transmittance according to the requirements. Also, adjust the graph plotting parameters to reflectance and transmittance.

f. Running the Analysis:

Click "Simple Analysis" during the operation, then click "Optimization Design" to perform the analysis. View the results by checking the data list and graph plotting parameters.

g. Repeated Testing:

Continuously test until the values on the smooth curve are approximately 100% and maintain a thin film layer thickness that meets the requirements.

4. Conclusion

The study successfully designed and realized a high-efficiency polarization beam splitter suitable for the visible light wavelength range of 400-700 nm and incident angles between 40° and 50°. The beam splitter achieved the design objective of near 100% reflectance for S-polarized light and near 100% transmittance for P-polarized light by optimizing the refractive indices, layer thickness, and multilayer structure of the thin film materials.The simulation results confirmed that the beam splitter provides high-efficiency polarization separation across the entire visible spectrum. This demonstrates the broad applicability of the design in advanced optical systems, including laser systems, optical instrumentation, and display technologies. The use of TFCale software proved to be an effective method for optimizing the design parameters, offering reliable and precise control over the optical

DOI: 10.54254/2753-8818/87/2025.20347

performance. This research provides a valuable reference for future work in thin-film polarization technologies.

5. Discussion

This study does not encompass the production and processing of the thin films; therefore, the production aspects are discussed below only in a theoretical context. The following work in sections 5.1.1–5.1.2 primarily refers to the literature in reference [9].

5.1. Preparation Procedure

5.1.1. Specimen Wiping

(1)For freshly polished specimens, use a mixture of alcohol and ether for wiping. Inspect under a 60W inspection lamp equipped with a condenser, typically using the breath fogging method.

(2)For specimens exposed to the atmosphere for extended periods, which may develop mold spots on the surface, use a cotton swab dipped in $CaCO_3$ powder for wiping. Rinse with clean water, then wipe with a mixture of anhydrous ethanol and ether. Finally, inspect under a 60W inspection lamp with a condenser and check using the breath fogging method.

5.1.2. Evaporation Technology

(1)Startup and Preheating:

Turn on the cooling water circulation, then the air compressor, and finally the power supply.

Press the mechanical pump start button 2-3 times to activate the mechanical pump, open the pre-valve, and then start the diffusion pump for preheating (preheat for approximately one hour).

(2)Filling the Evaporation Material and Loading the Workpieces:

Open the gas valve to fill the vacuum chamber. Once the chamber door opens, close the gas valve.

Clean the vacuum chamber, install or inspect the evaporation source, and fill the evaporation material.

Install the monitoring piece, activate the film thickness control system, and check for normal operation. Load the optical parts to be coated, then install the compensation shutter, press the workpiece rotation button, adjust the workpiece rotation speed, and close the vacuum chamber.

(3)Vacuum Pumping:

Close the pre-valve, open the low valve, and activate the vacuum gauge to start low vacuum pumping.

When the vacuum reaches approximately 5 Pa, close the low valve, open the pre-valve, and then the high valve to start high vacuum pumping.

When the high vacuum gauge shows a reading, activate the baking process and set the target temperature. Before evaporation, adjust the monochromator to the corresponding value and check the optical path for normality.

(4)Pre-Melting and Evaporation:

When the vacuum reaches approximately 10^{-3} Pa, pre-melt the material. During pre-melting (manual), do not increase the current too rapidly; gradually increase the beam current. The duration of pre-melting should be such that the outgassing from the evaporation material is minimal, MgF_2 does not splatter, and the material is fully melted.

After pre-melting, load the program from IC/5. When the vacuum reaches approximately 10^{-3} Pa, set the electron gun control to EXT (external control) and select crystal control on the touch screen. Press the Start button on IC/5 to begin evaporation. Monitor the film thickness control instrument

DOI: 10.54254/2753-8818/87/2025.20347

IC/5 and the optical control values, pressing the optical control button on the touch screen at the extrema. The evaporation process is completed at this point.

(5)Removing the Workpieces and Shutting Down:

Turn off the electron gun, baking process, high valve, and vacuum gauge. If the day's work is finished, turn off the diffusion pump.

Depending on the cooling status of the vacuum chamber, open the gas valve to open the chamber. Set the workpiece rotation speed to zero, press the workpiece rotation button, close the gas valve, and remove the coated optical parts.

After removing the workpieces, close the vacuum chamber, close the pre-valve, and open the low valve. When the vacuum reaches approximately 5 Pa, close the low valve and open the pre-valve.

After the diffusion pump cools (approximately one hour), close the pre-valve and turn off the mechanical pump.

Turn off the main power supply, air compressor, and cooling water circulation.

6. Error Analysis

The following work in sections 5.1–5.8 primarily refers to the literature in reference **[9]**.

6.1. Film Strength

Film strength is a crucial parameter for lens coatings and one of the most common sources of error in the coating process. Poor film strength manifests primarily as:

(1)Large areas of film peeling off when wiped or pulled with specialized tape.

(2)Spot-like film detachment when wiped or pulled with specialized tape.

(3)Spot-like or sheet-like film detachment after boiling for 15 minutes followed by tape pulling.

(4)Scratch marks after rubbing with a specialized rubber head with 1Kg force for 40 times.

(5)Cracks or fine network-like scratches on the film layer, whether wiped or not.

Causes of Poor Film Strength:

(1)Adhesion between the Substrate and the Film Layer:

Generally, in anti-reflective coatings, poor adhesion is the primary cause of weak films. During optical cold processing and cleaning, unavoidable harmful residues can adhere to the substrate surface. Additionally, the surface inevitably has some damaged layers due to processing. The impurities (such as water vapor, oil vapor, cleaning solution, wiping liquid, polishing powder, etc., with water vapor being the main one) that penetrate these damaged layers are difficult to remove completely, especially from hydrophilic and highly adsorptive substrates. When film material molecules accumulate on these impurities, adhesion is compromised, affecting film strength. Furthermore, substrates with poor hydrophilicity and low adsorption capability also exhibit poor adhesion to the film layer, affecting film strength. Chemically unstable glass substrates can develop corrosion or hydrolysis layers during processing, leading to poor adhesion and weak film strength when the film is deposited on these layers. Contaminants like dirt, oil stains, dust, and saliva spots on the substrate surface can also cause localized weak adhesion, resulting in poor film strength in those areas.

(2)Film Layer Stress:

The film formation process involves a transformation of material states, which inevitably results in stress within the film layer. In multilayer films, different materials exhibit varying stress levels—tensile stress, compressive stress, and thermal stress from both the film layer and the substrate. These stresses are detrimental to film strength, leading to susceptibility to abrasion or, in severe cases, causing cracks or fine network-like scratches. Although anti-reflective films typically exhibit less noticeable stress due to fewer layers, some glass substrates can still experience stress issues. High-

DOI: 10.54254/2753-8818/87/2025.20347

reflective and filter films with multiple layers are more prone to stress-related defects and require careful attention.

(3)Surface Hardness of the Outer Film Layer:

If the surface hardness of the outer film layer is low, it is prone to scratches during wiping.

(4)Other Factors:

Other causes of poor film strength include low vacuum levels (common in manually controlled systems), dirty vacuum chambers, and inadequate substrate heating. Additionally, the introduction of auxiliary gases can reduce the vacuum level, decreasing the mean free path of molecules and resulting in weak film adhesion. Therefore, the introduction of auxiliary gases must consider the outgassing of the film material. Thorough pre-melting and outgassing of the film material before deposition can prevent excessive vacuum reduction and thus maintain film strength.

(5)Film Peeling:

Although film peeling is a form of weak film adhesion, it differs slightly from the previously mentioned types. It mainly manifests as spot-like, edge, or localized peeling. The primary cause is contamination or impurities within the film.

6.2. Film Material Spots

Defective film material spots are a common issue in coating errors. In Japanese and Taiwanese companies, these spots are referred to as "spot holes." Essentially, film material spots are formed when large particles of film material evaporate along with the film material vapor and deposit on the substrate surface, creating raised spots. These spots can be isolated or, in severe cases, appear as clusters of fine points. Large particles can even damage the substrate surface. The evaporation characteristics of different film materials vary, particularly in their melting and evaporation temperatures.

(1)Sublimation Materials: These materials have a melting temperature higher than their evaporation temperature, evaporating directly from solid to gas.

(2)Non-sublimation Materials: These materials have a melting temperature lower than their evaporation temperature, transitioning from solid to liquid before evaporating into gas. Non-sublimation materials are most prone to film material spots because continued heating of the liquid film material causes boiling, during which bubbles can burst and increase the likelihood of splattering film material spots. Significant splattering can also occur during the pre-melting stage.

(3)Semi-sublimation Materials: These materials have melting and evaporation temperatures that are relatively close. They evaporate from solid to gas while partially melting.

The presence of film material spots is most likely with non-sublimation materials. Impurities or inconsistent melting and evaporation temperatures within the film material also contribute to the formation of these spots.

6.3. Film Color Variation

There are two types of film color variations (excluding color spots): one where the film color is inconsistent across the top, middle, and bottom of the entire coating, resulting in differing spectral test curves, and another where the color is inconsistent on a single piece.

(1)Inconsistency across the top, middle, and bottom (whole canopy variation): This is referred to as poor canopy (cover) uniformity or canopy difference. The main cause is issues with the uniformity correction plate (compensation plate).

(2)Deformation of the canopy plate: This is another cause of non-uniform film color, especially in older canopy plates that were initially uniform but have gradually become uneven. Deformation of the canopy plate can be the primary reason for this change.

DOI: 10.54254/2753-8818/87/2025.20347

(3)Inconsistent film material conditions: Particularly when sublimation and semi-sublimation materials are improperly positioned or have issues like pitting. This significantly impacts both whole canopy and single-piece uniformity. Manual pre-melting processes can exacerbate this issue, as individual operator techniques vary, leading to inconsistent material conditions.

For single-piece film color inconsistency:

(1)Severe substrate irregularities: Large differences in the curvature between the substrate and the canopy plate cause variations in the evaporation angle between the substrate's upper or lower normals and the evaporation source. This results in significant differences in film thickness across different parts of a single lens.

(2) Obstruction and contamination: The lens edges being blocked by the lens holder (disc edge) or contamination of the lens holder (disc) during evaporation can also cause film color variation.

6.4. Film Contamination (also known as White Acrylic)

As the name suggests, film contamination refers to dirt on the film layer. Contamination can occur inside or outside the film and can include dust particles, white haze, oil stains, fingerprints, and saliva spots (dust particles and white haze are listed separately).

(1)Dust Contamination:

Phenomenon: Dust particles can be present on the surface or inside the film layer. Some can be wiped off, while others cannot, potentially causing point-like delamination.

Analysis of Causes:

①Dirty Vacuum Chamber: Dust from the vacuum chamber’s bottom plate and protective plates can be carried onto the lenses by air turbulence when vacuuming starts, forming a layer of dust particles inside the film that cannot be wiped off and may cause point-like delamination.

②Dirty Lens Rings or Discs: Floating dust particles can adhere to the lenses under ion beam action, creating a dust particle layer inside the film that cannot be wiped off and may cause point-like delamination.

③Pre-existing Dust on Lenses: Dust particles present on the lenses before placing them in the canopy, which were not checked or cleaned beforehand, result in dust inside the film that cannot be wiped off and may cause point-like delamination.

④Post-Coating Environmental Contamination: Dust particles on the outside of the film are mainly caused by environmental pollution after coating, especially when the lenses are hot, making them more likely to attract dust that is difficult to remove.

⑤Dirty Environment at Vacuum Chamber Gas Inlet: Excessive initial gas flow, dirty gas filters, and high lens temperatures during gas intake can also cause dust contamination on the outside of the film.

⑥Human-Induced Dust Pollution: Dust contamination can occur both inside and outside the film due to operator actions.

⑦Dusty Work Environment: An excessively dusty environment contributes to contamination.

(2)External White Haze:

Phenomenon: After coating, a faint white haze appears on the surface, which worsens with wiping using acetone or mixed solvents. Wiping with cerium oxide can remove or reduce it, often referred to as "wipeable acrylic."

Analysis:

①Film Structure Issues: A loose columnar structure of the outer film layer or excessive roughness of the outer film layer.

②Large Evaporation Angle: Leading to a rough film structure.

DOI: 10.54254/2753-8818/87/2025.20347

③Temperature Difference: Significant temperature difference between the inside and outside of the lens when removed from the canopy.

④Humidity: Humidity in the storage environment after removing the lens from the canopy.

⑤Heavy Moisture During POLYCOLD Thawing: Excessive moisture inside the vacuum chamber during POLYCOLD thawing.

⑥Incomplete Oxygenation During Evaporation: Leading to an uneven film structure.

⑦Interlayer Stress: Stress between different film layers.

(3)Internal White Haze:

Phenomenon: White haze forms inside the film and cannot be removed by wiping.

Analysis of Possible Causes:

①Dirty Substrate: Residues from previous processes adhered to the substrate.

②Surface Corrosion of the Lens: Corrosion and pollution on the lens surface.

③Mismatch Between Film Materials: Incompatibility between different film materials or between the film material and the substrate.

④Insufficient Oxidation: Inadequate oxygenation of oxide materials.

⑤Initial Layer of Zirconium Oxide: Potentially causing white haze on some substrates.

⑥Humidity Contamination Before Coating: Moisture pollution of the substrate before entering the canopy (after cleaning).

⑦Poor Cleaning or Wiping: Inadequate cleaning or wiping, leaving marks or residues.

⑧Dirty Vacuum Chamber: Excessive moisture inside the vacuum chamber.

⑨High Environmental Humidity: Leading to increased risk of contamination.

6.5. Color Spots

Color spots (also known as film color acrylic or ablation) refer to local variations in the film color on the lenses, generally in irregular patterns. There are two types: internal color spots (including film layer color spots) and external color spots. Sometimes, regular localized areas (such as the center of concave lenses or ring-shaped areas) exhibit color variations.

Causes of Color Spots:

(1)Local Refractive Index Variation:

Film color reflects the spectral characteristics of the thin film. The design and achievement of these spectral characteristics are based on a substrate with a specific refractive index. If the local refractive index of the substrate changes, the local spectral characteristics of the film layer also change, resulting in internal color spots.

During and after coating, various reasons can cause local refractive index variations in the film layer, forming color spots within or outside the film. External color spots are usually lighter and can be polished away with cerium oxide or calcium carbonate powder. In contrast, internal or bottom-layer color spots caused by local refractive index variations cannot be removed this way.

An effective method to differentiate between internal and external color spots is to use cerium oxide or calcium carbonate powder for polishing. The treatment strategies for internal, film layer, and external color spots differ.

Sources of Internal Color Spots:

①Local Refractive Index Change on Substrate: Mostly caused by local substrate corrosion, forming a very thin low-refractive-index layer.

Processing Equipment and Methods: Local variations may arise from tooling, fixtures, and processing methods during the previous stages, leading to color spots of various sizes. Such spots typically have regular shapes, consistent locations, and clear boundaries.

DOI: 10.54254/2753-8818/87/2025.20347

②Handling, Transport, and Storage: Some substrates, like H-ZK9, have poor chemical stability and are susceptible to moisture and acid, leading to corrosion during handling, transport, and storage. If the period between pre-processing and coating exceeds five hours, internal color spots can form, especially in reflective and infrared cut-off films. These spots may not be initially visible but can appear after a few days, rendering the lens defective.

③Incomplete Cleaning Post-Grinding and Polishing: Residual polishing powder and liquids can harden on the lens surface, causing corrosion or pollution that cannot be removed by cleaning or wiping. This manifests as color spots after coating.

④Uncontrolled pH of Polishing Liquids: Mismatched pH values can affect the chemical stability of the lenses between the grinding and coating processes.

(2)Formation of Film Layer and External Color Spots:

①Post-Coating Impurities: Contaminants infiltrating the gaps in the film layer post-coating can alter the local refractive index, forming external color spots.

②High Substrate Temperatures: During coating, excessively high temperatures of some high-refractive-index substrates can cause local refractive index variations in the film layer or at the film-substrate interface, resulting in color spots.

③Thin and Unstable Film Layers: Incompatible matching of film systems can lead to color spots if some film layers are too thin and crystalline structures are unstable.

④Mismatch Between Film Materials and Substrate: Poor compatibility between the film material and substrate can also cause film layer color spots.

⑤Micro Oil Backflow in Equipment: Micro oil backflow in the coating equipment can form thin oil spots on the lens or film layer, leading to color spots. These spots typically exhibit reduced film strength.

6.6. Spectral Characteristics

Spectral characteristic issues (poor spectral performance) are common problems in optical thin film products. Poor spectral characteristics mean that the spectral reflectance (transmittance) curve does not meet the technical requirements of the product, which is a functional defect that must be strictly controlled during production.

Causes of Poor Spectral Characteristics:

(1)Film System Design:

The design tolerances for film thickness and refractive index are too small. If the spectral curve during trial production is on the edge of the technical requirements, even slight deviations in manufacturing can lead to poor spectral performance.

(2)Discrepancies in Refractive Index:

The designed refractive index of the film material differs from the actual refractive index, or the refractive index has changed.

(3)Center Wavelength (Film Thickness) Variance:

There is a difference between the actual coated center wavelength (film thickness) and the desired center wavelength (film thickness), or it has changed (Tooling value, also known as F value, deviation).

(4)Manufacturing Errors:

Errors such as using the wrong film material, incorrect programming, or not closing the shutter during pre-melting.

(5)Changes in Process Conditions:

Changes in vacuum level, oxygen intake, heating temperature, evaporation rate, substrate rotation speed, ion assistance conditions, etc.

DOI: 10.54254/2753-8818/87/2025.20347

(6)Material Changes:

Differences in the optical and chemical properties of the same type of optical material produced by different manufacturers (or different batches from the same manufacturer). Sudden changes in materials during production (especially in large-scale production) without verification can lead to poor spectral performance.

(7)Variations in Comparison Plate Surface Properties:

Changes in the surface properties of the comparison plate used for spectral testing can cause poor spectral performance. This issue, often overlooked, is common, especially if a high refractive index comparison plate has formed a corrosion layer on its surface, acting like a very thin anti-reflective film. This can make the spectral test results inaccurate and unstable. Comparison plates are often stored longer and in less controlled environments than lenses, exacerbating the problem.

(8)Poor Stability of Equipment Process:

Issues such as inconsistent pumping speed, significant equipment vibration, shaking of the test plate or crystal, inconsistent rotation, deformed umbrella plates, large temperature measurement errors, and unstable heating power.

(9)Quartz Crystal Oscillator Control:

The quality and lifespan of the crystal oscillator, and changes in activity value. The sensitivity of a crystal oscillator at the beginning of its use differs from its sensitivity after a period (e.g., after coating 3 batches of 6-layer anti-reflective films), leading to shifts in the overall curve.

(10)Poor Water Cooling of Crystal Control Probe:

Causing instability and unreliability in crystal control, resulting in inaccurate film thickness control.

(11)Differences Between Immediate and Delayed Testing:

Spectral characteristics can differ between immediately after coating and after a period.

(12)Post-Coating Refractive Index Changes:

The refractive index of some film materials changes after coating (depending on coating conditions and film layer matching), affecting spectral characteristics.

(13)Substrate Refractive Index Variations:

Some substrate materials form a very thin low-refractive index layer on the surface after ultrasonic cleaning, affecting spectral characteristics and film color.

(14)Manual Light Control:

In non-automatic control, inappropriate light intensity settings or changes in film material refractive index causing deviations in light intensity settings, leading to spectral characteristic deviations or instability.

(15)Corrosion Layer on Monitoring Plate in Light Control:

Affects light control values.

(16)Unstable Light Signal in Light Control:

Issues like voltage fluctuations, poor contact, and electronic component problems affecting accuracy and stability.

(17)Thin Film Layers in Light Control:

Some film layers are too thin (especially the first layer), not reaching a peak value, leading to inaccurate light control.

(18)Human Error in Manual Light Control:

Errors in human judgment during manual light control.

6.7. Edge Chipping and Cracking Defects

In general, during the coating process, the substrate is heated. Since the substrate is mounted within metal (aluminum, copper, stainless steel) rings or disks, the difference in thermal expansion

DOI: 10.54254/2753-8818/87/2025.20347

coefficients between the lens ring or disk and the lens (substrate) can cause edge chipping or cracking during the cooling process. Some large lenses may experience high temperatures when exiting the coating chamber. The significant temperature difference between the lens and room temperature can induce thermal stress, leading to lens cracking or edge chipping. Additionally, certain shapes of beveled edges on parts can cause them to get stuck in the rings, resulting in edge chipping.

6.8. Scratches (Coating Damage)

Scratches refer to lines or marks on the coating surface, with internal scratches called "scratches" and external scratches called "coating damage." This issue is a persistent problem in coating quality improvement. Despite understanding the causes and improvement methods, it remains challenging to completely eradicate.

Causes:

(1)Internal Scratches:

①Residual Appearance Defects from Previous Processes: Some scratches may not be easily detected before coating. They might not be noticeable during pre-coating inspections but become evident after the coating process.

②Operational Errors: Scratches on lenses caused by mistakes during various operational processes.

③Dense Placement of Lenses: Lenses placed too closely together can bump into each other during handling, causing scratches.

④Damage from Placement Tools or Packaging Materials: Scratches on lens surfaces caused by the tools or materials used for placing and packaging the lenses.

⑤Ultrasonic Cleaning Damage: Scratches resulting from the ultrasonic cleaning process.

(2)External Scratches (Coating Damage):

①Damage from Placement Tools or Packaging Materials: Coating damage caused by the tools or materials used for placing and packaging the lenses.

②Post-Coating Ultrasonic Cleaning Damage: Coating damage resulting from the ultrasonic cleaning process after coating.

References

[1] *Macleod, H. A. (2001). Thin-Film Optical Filters. CRC Press.*
[2] *Dobrowolski, J. A. (1995). "Optical coatings: A user's guide for design and application." Applied Optics, 34(22), 4327-4338.*
[3] *Southwell, W. H. (1983). "Gradient-index antireflection coatings." Optics Letters, 8(11), 584-586.*
[4] *Yeh, P., & Yariv, A. (1980). Optical waves in layered media. Wiley.*
[5] *Zhang, L., & Li, S. (2017). "Polarization beam-splitter design based on multilayer coatings." Optics Express, 25(14), 16308-16316.*
[6] *Dobrowolski, J. A. (1995). "Optical coatings: A user's guide for design and application." Applied Optics, 34(22), 4327-4338.*
[7] *Born, M., & Wolf, E. (1999). Principles of Optics. Cambridge University Press.*
[8] *Hecht, E. (2002). Optics (4th ed.). Addison Wesley.*
[9] *Fu Xiuhua, Zhang Jing, Fu Xinhua. Optical Thin Films and Technology Laboratory ManualM. Changchun: Changchun University of Science and Technology, August 2011.*